April 2008 Volume 4 Issue 3

Trade Science Inc.

Materials Science

An Indian Journal

Full Paper

MSAIJ, 4(3), 2008 [217-224]

Influence of maleic anhydride-methacrylic acid copolymer on calcium scales cyrstallinity and morphology

Shakkthivel Piraman*, Ramalakshmi Shakkthivel

Department of Chemical Engineering, Yonsei Unniversity, Seodaemun-Ku, Seoul-120 749, (KOREA)

Tel: +82-2-2123 3554 (Extn.34); Fax: +82-2-312 6401

E-mail: apsakthivel@yahoo.com

Received: 27th December, 2007 ; Accepted: 1st January, 2008

ABSTRACT

The formation of calcium carbonate and calcium sulphate scales in cooling water was mitigated by adding poly(maleicanhydride-co-methacrylic acid) polymer. Maleic anhydride- methacrylic acid copolymer (Man-MAA) was synthesized by adopting bulk polymerization procedure. The synthesized Man-MAA copolymer was characterized through Ultraviolet-visible (Uv-visible) spectroscopy and Fourier transformation Infrared (FTIR) spectroscopy methods. The viscosity of the polymer was only 1.1CPS, which is more responsible for the antiscaling property of the polymers. Antiscaling performance of this polymer was evaluated by performing chemical screeing test, constant potential electrolysis and electrochemical impedance techniques. The addition of Man-MAA polymer is not altered the crystal structure of the either $CaCO_3$ or $CaSO_4$ crystals, it affects only the crystal growth and thus much reduced size was the result, which is evident from the SEM and XRD results. The Man-MAA polymer has offered very good antiscaling property in both of the brines.

KEYWORDS

Antiscalant;
Maleic anhydride-co-methacrylic acid polymer;
Constant potential electrolysis;
EIS;
SEM;
XRD.

INTRODUCTION

Often industrial plants or domestic equipments suffer from technical or commercial problems due to calcareous scale deposits from water sources[1,2]. It is found that calcium carbonate scale to be a predominant foulant of heat transfer surfaces. Normally, the scales are found to consist of primarily carbonates, sulphates, hydroxides, phosphates and silicates of alkaline earth metals particularly calcium and magnesium. The problem of scale formation is intensified at higher temperatures because of the reversal of temperature-solubility characteristics of these minerals in water[3]. The characteristics of the scale formed depend on a number of parameters, including the concentrations of lattice forming ions, the amount of dissolved and suspended solids, the pH and flow properties of the solution, the rate of evaporation and the operating temperature, and pressure of the system. Scale facilitates the corrosion of metal surfaces, restricts fluid flow, and reduces the quantity of heat transferred across the metal fluid boundary. As a consequence the scaling is a major operational problem, and the heat exchanger units have to be cleaned from time to time by chemical and / or mechanical means

to maintain the optimum output. This invariably adds to operation cost[4]. Many of the naturally occurring polymers have been tried as crystal modifiers and dispersants of microcrystallites[5,6]. However, many of them are found to oxidize at high temperatures. More recently, substoichiometric compounds of synthetic water soluble low molecular weight polymers and co-polymers that are thermally stable and provide antiscaling properties have been widely employed in the protection of heat exchanger surfaces[7-10]. Antiscalants such as phosphonate family (Permatreat 191) and polymers which are superior crystal modifiers (Flocon 100) have been studied extensively for their field applicability[11]. Commercially available antiscalants efficiency was assessed for their real field applications in different plants[12,13]. The effect of poly(ethylene glycol) and poly(propylene glycol) based polymers on the calcium carbonate scales have been reported[14]. Acrylonitrile copolymer of Acrylic acid and Methacrylic acid have been tried as antiscalant for cooling water treatment[15]. The antiscalant effectiveness in retarding the mineral salt (Gypsum) have been tried through dual use of turbidity and calcium potential measurement[16]. In the present work one such copolymer namely maleic anhydride-methacrylic acid has been tried as an antiscalant for the scale of calcium carbonate and calcium sulphate brines.

EXPERIMENTAL

Polymer synthesis and characterization

Polymerization of 1,2 disubstituted ethylenes is very difficult[17] due to the low reactivity of monomers towards propagating polymer radical expecially because of the steric hinderance of substituents at 1,2 position of the double bond. However, it undergoes copolymerization easily with vinyl monomers. Maleic anhydride-methacrylic acid copolymer was synthesized at 70ºC with a reaction time of an hour. Hydrogen peroxide was used as the initiator. After polymerization, the pendant acid groups were neutralized, and precipitated from ethyl alcohol. The synthesized Man-MAA copolymer was characterized through Uv-visible and FT-IR spectrometric techniques using Schimadzu UV, PC-2401, Uv-visible spectrophotometer and PERKIN ELMER FT-IR spectrometer, Paragon model 500.

Evaluation of antiscalant

1. Chemical screening test

The calcium carbonate and calcium sulphate brines were prepared as per NACE standard procedure[18,19]. In the case of carbonate brine the effective concentration of Ca^{2+} taken was to be 300ppm and it was 2000ppm in the case of sulphate brine. 100ml of the test solution was taken in different stopper airtight glass cells along with varying concentration of scale inhibitor (1-20ppm). A blank solution (without any inhibitor addition) was also prepared. The test cells were capped tightly and kept in a constant temperature water bath for 6 hours digestion and 12 hours allowed for settling. After the test period, the cells were cooled and the calcium ion concentration retained in each solution (Total hardness) was determined by EDTA titration. The test was carried out at different temperatures 50-80ºC and at various pHs (7.0-8.5) with a step value of 5ºC and 0.5 pH respectively.

2. Constant potential electrolysis

Electrochemical test was carriedout using Versastat-II. A three electrode cell assembly was used for carrying out the tests. A platinum foil of area 1x1 cm^2 was used as the working electrode. Counter electrode was also a platinum foil of nearly double the area as that of the working electrode. A saturated calomel electrode (SCE) was used as the reference electrode through out the study. The test solution was the dilute brine solution as prepared for chemical screening tests containing 300ppm of calcium carbonate brine hardness. Various polymer dosage levels (1-20ppm) were added to the test solution. The pH was maintained at 8.0 and the experiment was run at room temperature. A constant potential of -1.2V Vs SCE was applied to the test electrode[20,21] and the change in current density values were followed with time for 30 minutes. After each experiment the working electrode was cleaned with funning nitric acid and rinsed with double distilled water.

3. A.C impedance technique

A three electrode cell assembly used for the impedance measurements was the same as that used for the constant potential electrolysis. The impedance measurements were carried out using EG & G, PAR model 398 Electrochemical impedance spectrometer in the

frequency range of 100kH-100mHz,. A condition potential of -1.2V Vs SCE was applied for 30 minutes before carrying out the experiments for maintaining the scaling conditions in the case of carbonate brines. This electrochemical deposition method provides controlled and reproducible deposition of calcium carbonate each time[21-23]. After completion of the scale formation the impedance measurements were carried out.

4. Surface examination techniques

The morphological changes in the $CaSO_4$ and $CaCO_3$ crystal structure with Man-MAA copolymer were examined through SEM and XRD surface examination techniques. SEM photographs were taken by JOEL JSM 840A scanning microscope and JOEL 8030 X-ray diffractometer was used to take the XRD spectra.

RESULTS AND DISCUSSION

Characterization

The molecular weight of the polymer was assessed through viscosity measurement by Efflex viscometer. The viscosity for water is 1.0 cps and for Man-MAA polymer was 1.1cps only. Viscosity being the index of the molecular weight indicates the synthesized Man-MAA polymer molecular weight was low.

UV-visible spectra were taken for homo and copolymers. The spectra help to identify the formation of copolymer distinct from the homopolymer. The expected structure of synthesized Man –MAA copolymer is

Man-MAA polymer structure

The Uv-visible spectra taken for maleic anhydride-

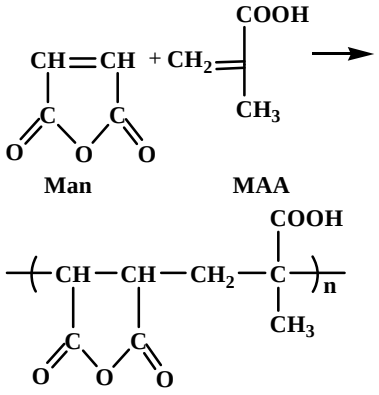

Man-MAA copolymer

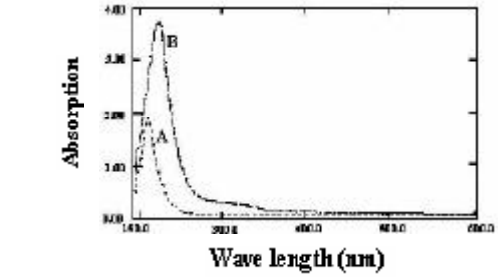

Figure 1: Uv-visible spectra of poly(methacrylic acid) (A) and Man-MAA copolymer (B)

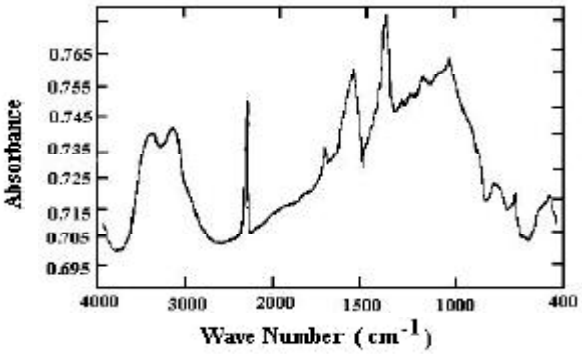

Figure 2: FT-IR spectrum of Man-MAA copolymer

methacrylic acid copolymer and polymethacrylic acid given in figure 1. The copolymer gives absorption peak at 318nm that corresponds to C=O present in the anhydride group, and a peak at 223.5nm corresponds to C=O of the carbonyl group of the carboxylic acid[24,25]. Figure 2 is the FT-IR spectrum of Man-MAA copolymer. The peak at 1585cm^{-1} is assigned for COO^- stretching vibration present in vinyl unit. Absorption peak at 1780cm^{-1} is for C=O stretching vibration in five membered cyclic anhydride. The CH_2 scissoring deformation vibration peak appears at 1401cm^{-1}[24, 25].

Chemical screening test

The antiscaling efficiency of the polymer towards calcium carbonate scale inhibition was determined by chemical screening method and electrochemical techniques. The efficiency of Man-MAA polymer on inhibiting calcium sulphate scale formation was found only by chemical screening test as the electrochemical conditions do not stimulate any sulphate scale formation. The antiscaling efficiency of the polymer at different dosage level was determined using NACE standard procedure and the results are presented both for carbonate and sulphate scales at different pH and temperatures in TABLE 1 and 2 respectively. It is observed

Full Paper

TABLE 1: Antiscaling efficiency of Man-MAA copolymer on calcium carbonate scale (300ppm hardness) at different temperatures and pH' s through chemical screening test

Sl.no.	Temp. (°C)	Dosage level(ppm)	Percentage efficiency			
			pH 7.0	pH 7.5	pH 8.0	pH 8.5
1	50	Blank	-	-	-	-
2		1	89	85	83	50
3		2	95	95	100	60
4		5	100	100	100	65
5		10	100	100	100	30
6		20	100	100	100	25
1	60	Blank	-	-	-	-
2		1	85	77	72	55
3		2	96	82	79	61
4		5	100	99	96	72
5		10	100	100	100	50
6		20	100	100	100	45
1	70	Blank	-	-	-	-
2		1	80	78	63	50
3		2	95	95	88	78
4		5	100	99	95	56
5		10	100	100	99	69
6		20	100	100	100	57
1	80	Blank	-	-	-	-
2		1	71	65	55	40
3		2	83	80	71	37
4		5	98	99	82	47
5		10	100	100	89	48
6		20	100	100	93	52

TABLE 2 : Antiscaling efficiency of Man-MAA copolymer on calcium sulphate scale (2000ppm hardness) at different temperatures and pH' s through chemical screening test

Sl.no.	Temp. (°C)	Dosage level(ppm)	Percentage efficiency			
			pH 7.0	pH 7.5	pH 8.0	pH 8.5
1	50	Blank	-	-	-	-
2		1	99	94	92	83
3		2	100	100	100	96
4		5	100	100	100	100
5		10	100	100	100	100
6		20	100	100	100	100
1	60	Blank	-	-	-	-
2		1	88	85	73	70
3		2	99	98	97	95
4		5	100	100	100	100
5		10	100	100	100	100
6		20	100	100	100	100
1	70	Blank	-	-	-	-
2		1	73	71	44	40
3		2	94	90	82	75
4		5	100	100	100	100
5		10	100	100	100	100
6		20	100	100	100	100
1	80	Blank	-	-	-	-
2		1	63	55	50	50
3		2	93	91	83	70
4		5	100	100	100	99
5		10	100	100	100	100
6		20	100	100	100	100

that in the case of carbonate scale as the concentration of the polymer increases the efficiency increases in the pH range of 7-8. However, the efficiency decreased with increasing temperature in the lower dosage levels upto 5ppm. At higher dosage levels, beyond pH 8.0 the efficiency of the polymer is found to decrease gradually. The same observations are noted for calcium sulphate scale also except that at higher pH of 8.5 and higher dosage levels, the polymer acts effectively as a dispersant.

Scale inhibitors function in substoichiometric amounts is by interfering in the nucleation and / or the crystal growth processes. The inhibitor is adsorbed at the active sites of the nuclei or microcrystalline surfaces, blocking or restricting further growth. As a result, the onset of crystallization can be delayed and crystallization rates are reduced. Crystal habit and size can also be affected and this explains the mechanism of inhibition of scaling by the polymer.

Constant potential electrolysis

Accelerated scale deposition on a metal surface can be conveniently carried out by electrochemically depositing calcium carbonate from calcium containing water by applying suitable potential at which the dissolved oxygen is reduced[26]. The same phenomenon is also addressed in cathodically protected metallic surfaces in sea water[22,26,27]. The deposition of calcium carbonate is detected and reported by following the decrease of oxygen reduction limiting current due to the progressive coverage of scale on the metal surface with time. A characrteristic current-time curve obtained by polarizing the electrode in 300ppm Ca^{2+} ions containing water at the reduction potential of oxygen (-1.2V Vs SCE) show two characteristic parts, sudden rapid decay followed by a slowly decreasing current value with increasing time, which can be explained as follows[19,22,27-29].

The electrochemical reduction reaction that usually takes place on a metal surface immersed in neutral medium is the reduction of oxygen,

$$O_2 + H_2O + 4e^- \rightarrow 4OH^-$$

and in minor cases, evolution of hydrogen,

$$2H_2O + 2e^- \rightarrow 2OH^- + H_2$$

The production of OH^- ions in either cases results in an increase in pH of the electrolyte adjacent to the metallic electrode surface. In water systems, the pH is controlled by the carbon dioxide equilibrium system, which can be given as,

$$CO_2 + H_2O \rightarrow H_2CO_3$$
$$H_2CO_3 \rightarrow H^+ + HCO_3^-$$
$$HCO_3^- \rightarrow H^+ + CO_3^{2-}$$

In such a system, production of OH^- ions on the electrode surface changes the inorganic equilibria and enhances the buffering reaction,

$$OH^- + HCO_3^- \rightarrow H_2O + CO_3^{2-}$$
$$CO_3^{2-} + Ca^{2+} \rightarrow CaCO_3$$

The higher concentration of OH^- ions increases the concentration of CO_3^{2-} ions; as a result, the formation of $CaCO_3$ is promoted. This calcareous deposit block the active surface area available for the electrochemical reaction to take place. Thus increasing calcareous deposit formation decreases the rate of oxygen reduction by functioning as an insulating layer for oxygen diffusion[30]. In the characteristics curve obtained, the sudden decay in the current density may be accounted as due to the depletion of oxygen for reduction on the electrode surface. The second part, slowly decreasing current with time may be due to the increasing coverage of calcium carbonate deposit on the electrode surface.

For this type of current-time curve, Gabrielli et al.[23] have suggested a calculation procedure to determine the two parameters, scaling time (t_s) and residual current (I_R). The scaling time can be defined as the time required for the full coverage of the electrode surface with insulating scale[31]. After the full coverage of the electrode surface no further oxygen can diffuse across the deposit and therefore the cathodic reduction reaction rate is limited, and an almost constant current value exists thereafter (residual current)[32]. The change in scaling time and residual current in the presence of the Man-MAA polymer at pH 8.0 are shown in figure 3 and in TABLE 3. This indicates, with increasing polymer addition increases the I_R and t_s values that is the polymer restrict the formation of calcareous deposit on the surface of the electrode. With the presence of the polymer additives that are capable of inhibiting or retarding or modifying the calcareous deposit formation, no or less deposit formation or delayed deposit formation or less adherent deposit results. As a consequence,

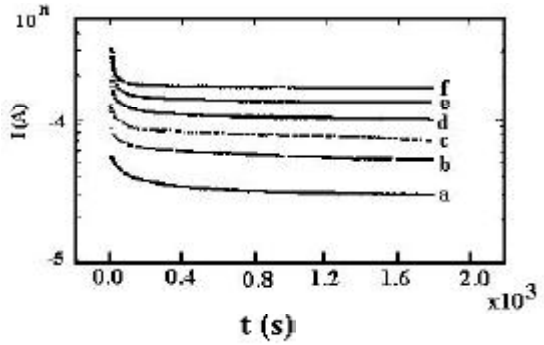

Figure 3: Current-time curve for calcium carbonate brine containing 300ppm of Ca^{2+} ions with the addition of Man-MAA obtained through constant potential electrolysis(a) Blank (b) 1ppm, (c) 2ppm, (d) 5ppm, (e) 10ppm and (f) 20ppm

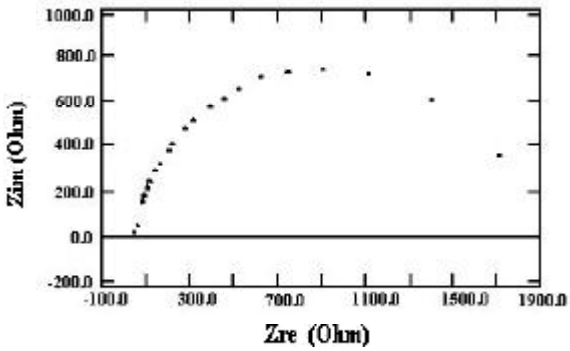

Figure 4: Nyquist plot obtained after $CaCO_3$ scaling on the Pt electrode immersed in calcium carbonate brine containing 300ppm of Ca^{2+} ions

TABLE 3: Scaling time and residual current for calcium carbonate scaling (300ppm of hardness) obtained from constant potential electrolysis at pH 8.0 with different dosage levels of Man-MAA polymer

Sl.no.	Dosage level (ppm)	Residual current (μA)	Scaling time(Sec.)
1	Blank	34.43	662
2	1	62.22	905
3	2	82.48	1206
4	5	108.81	1455
5	10	137.50	1579
6	20	173.90	1742

the scaling time and residual current values are found to increase.

Impedance spectroscopy

Gabrielli et al.[23] have recorded electrochemical impedance spectra during scaling process on a platinum electrode immersed in calcium ions containing water. In the present study, impedance spectra were recorded after complete formation of scale on the surface of the

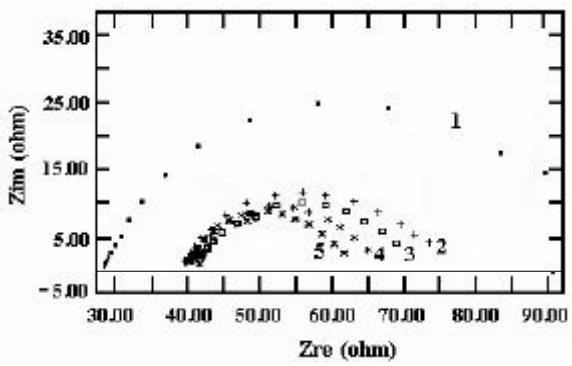

Figure 5: Electrochemical impedance spectrum for calcium carbonate scale in carbonate brine with different concentration of Man-MAA copolymer (a) 1ppm, (b) 2ppm, (c) 5ppm, (d) 10ppm and (e) 20ppm

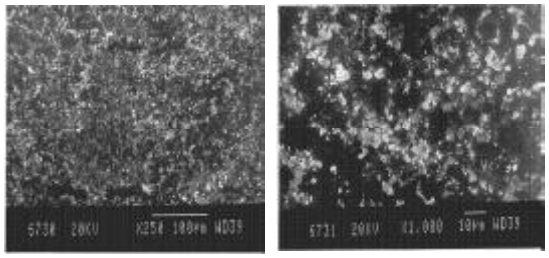

Figure 6: SEM photographs for calcium carbonate with the addition of Man-MAA copolymer at different magnifications (a) x 250 (b) x 1,000

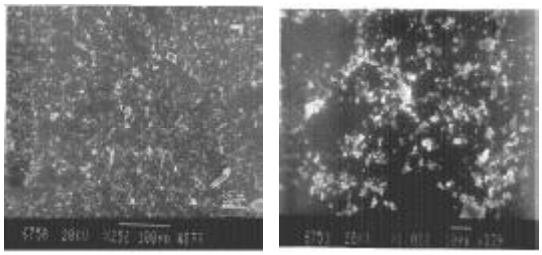

Figure 7: SEM photographs for calcium sulphate with the addition of Man-MAA copolymer at different magnifications (a) x 250 (b) x 1,000

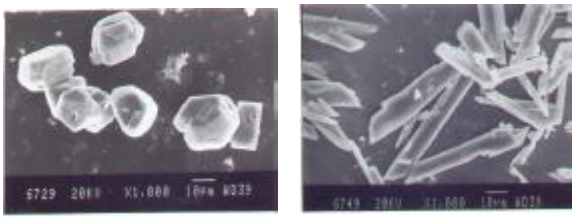

Figure 8: (a) SEM photograph for calcium carbonate crystal; (b) : SEM photograph for calcium sulphate crystal (a) x 250 (b) x 1,000

electrode immersed in 300ppm of hard water at a representative pH of 8.0 by impressing -1.2V vs SCE for

TABLE 4 : 2θ, d and I/I_0 values for calcium carbonate crystal and with the addition of Man-MAA copolymer

Calcium carbonate			Calcium carbonate with Man-MAA		
2θ	d	I/I_0	2θ	d	I/I_0
32.60	2.744	100	32.30	2.769	100
46.30	1.959	29	46.10	1.967	16
57.30	1.607	15	57.10	1.612	7
67.10	1.394	7	66.80	1.399	9
76.10	1.250	10	75.90	1.253	8

a duration of 30 minutes. The results are presented in figure 4. Nyquist plots for $CaCO_3$ scale with the addition of Man-MAA polymer are presented in figure 5. At higher frequency region, semicircle plots were obtained, which were taken for calculation. The R_t values for blank is 2100Ω/cm^2, however, with the addition of polymer R_t values decreased to only 21Ω/cm^2 for 20ppm Man-MAA addition. The impedance diagrams can be attributed to the electron transfer reaction limited by mass transport on a scale covered surface in the case of control and free surface in the case of polymer treated brine[33,34]. While increasing the addition of polymer dosage, the R_t values are decreased and C_{dl} values are increased. The change in double layer capacity values are related to dielectric nature of the scale formed.

Scanning electron microscope

The effect of the polymeric antiscalant on calcium carbonate and calcium sulphate scale morphology was examined through SEM study. The crystal habits and modifications brought about by Man-MAA copolymer on $CaCO_3$ and $CaSO_4$ with different magnifications are presented in figures 6-8.

The SEM photograph for the calcium carbonate scale is presented in figure 8a. Calcite crystals are formed in block like particles of cubic shape[28,33] or as entangled or elongated rhombohedral[20,34]. The changes in crystal morphology of the scale deposited in the presence of the polymer is presented in figures 6a and 6b. The distortion in the crystal morphology of the $CaCO_3$ scale by the Man-MAA is evident. The presence of the polymer in the brine decreased the amount of crystals formed on the surface[35].

SEM photographs for calcium sulphate without and with the presenc of the polymer are presented in figures 8b, 7a and 7b. Under the circumstances, among the

TABLE 5: 2θ, d and I/I_0 values for calcium sulphate crystal and with the addition of Man-MAA copolymer

Calcium sulphate			Calcium carbonate with Man-MAA		
2θ	d	I/I_0	2θ	d	I/I_0
11.90	7.431	100	12.00	7.369	23
21.00	4.227	18	21.10	4.207	27
23.70	3.751	40	29.50	3.025	22
29.40	3.035	27	32.10	2.786	100
32.10	2.786	6	33.90	2.642	15
35.70	2.513	4	43.80	2.065	11
36.90	2.434	10	45.90	1.975	60
41.00	2.199	4	57.00	1.614	23
45.70	1.984	6	66.70	1.401	9
48.20	1.886	8	75.70	1.255	18
50.60	1.802	10			
57.10	1.612	3			
69.00	1.360	2			

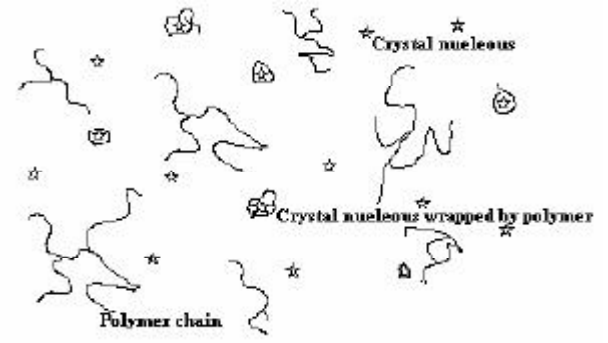

SCHEME 1: Schematic representation of scale inhibition through polymer wrapping

three forms of $CaSO_4$ crystal, the crystal habit corresponds to that of dihydrate crystal. These crystals are reported as thin tubular cells exhibiting monoclinic symmetry[36-38]. The total $CaSO_4$ scale shape (tubular cell) is completely absent in the presence of the polymer.

X-ray diffractometry

The scales of $CaSO_4$ and $CaCO_3$ were examined through XRD studies. The effect of the polymer on the scale structure was studied and the resulting data are given in TABLES 4 and 5. In the case of $CaCO_3$ scale the 'd' and "θ" values conform to the structure of calcite crystals as has been reported earlier[39]. With the presence of the Man-MAA polymer, the crystal structure of the calcite crystal have not been altered, confirmed from "d", "θ" and intensity values, but only the crystal habit or morphology is changed as evident from SEM studies[14]. For calcium sulphate scale, the structure is proved to be $CaSO_4$. $2H_2O$[40] and here also with the presence of the polymer only the crystal morphology is changed and there is no change in the crystal parameters.

Mechanism of scale inhibition

The mechanism of the scale inhibition is that the impurities get adsorbed on the growth sites of the nuclei, keeping them in the embryo stage and thus preventing their further growth and dispersed them[41]. According to Rolfe[42] the additive molecules where large, are easily able to wrap around the nucleus surface and effectively protect them from any further growth. The following schematic diagram represents how the polymer prevents the scale growth by adsorption (SCHEME 1).

The adsorbed polymer molecules not easily desorbed and act as immobile impurities on the crystal surface and inhibit crystal growth by reducing the rate of step movement (surface diffusion). The adsorbed polymer increases the electrostatic field around the particles[43], so that the double layer repulsion would also contribute to the prevention of coagulation. The scale inhibitors function in substoichiometric amounts by interfering in the neucleation and/or the crystal growth process through adsorption at the active sites blocking or restricting further growth[44]. The process of precipitation inhibition by the polymers must involve a step of polymer-nucleus association as the vital step.

CONCLUSION

The low molecular weight maleic anhydride-methacrylic acid copolymer is found to be a best antiscalant both for calcium carbonate and sulphate brines at dosage level of 5ppm and above. In the case of carbonate scale, the polymer is found to act as coagulant at higher dosage levels (20ppm and above) at higher pH (<8.5). The electrochemical techniques namely constant potential electrolysis and impedance spectroscopic techniques also reveal the trend of the chemical screening test. The crystals formed in this study were calcite crystal in $CaCO_3$ brine and calcium sulphate dihydrate crystal in the case of sulphate brine. The SEM and XRD results show the polymer restricts/retards the scales growth but no alterations in the crystal structure. Hence

this polymer can be used safely in the industries under optimum operational conditions.

REFERENCES

[1] G.F.Hays, P.A.Thomas, B.L.Libutti; Proc. Engineering Found. Conf. Pennsylvania, Engineering Foundations, New York, **(1982)**.

[2] H.Z.Schesinger; Tech.Phys., **12**, 33 **(1931)**.

[3] Z. Amjad; J.Colloids and Interface Science, **123**, 2 **(1998)**.

[4] E.Senogles, W.O.S.Doherty; CRC Press, Inc., **(1996)**.

[5] F.C.Welch; Am.Ceram.Soc., **6**, 1197 **(1983)**.

[6] H.F.Buckely, Crystal Growth, John Wiley & Sons, New York, **(1951)**.

[7] J.S.Gill, S.P.Rey, J.H.Wuernik; U.S.Patent, **4**, 933 090 **(1990)**.

[8] D.H.Emmons, FR.W.Dodd, M.A.Kinsella; U.S. Patent, **5**, 167-828 **(1992)**.

[9] L.A.Perez; Canadian Patent, **2**, 083-453 **(1993)**.

[10] L.L.Wood, U.S Patent, **5**, 286-810 **(1994)**.

[11] M.Al-Shammiri, M.Safar, M.Al-Dawas; Desalination, **128**, 1 **(2000)**.

[12] O.A.Hamed, M.A.K.Al-Sofi, M.Imam,; K.B. Mardouf, A.S.Al-Mobayed, A.Ehsan; Desalination, **128**, 275 **(2000)**.

[13] A.Plottu-Pecheux, B.Houssais, C.Democrate, D. Gatel, C.Parron, J.Cavard; Desalination, **145**, 273 **(2002)**.

[14] P.Kjellin; Colloids and Surfaces A: Physicochem. Eng.Aspects, **212**, 19 **(2003)**.

[15] P.Shakkthivel, R.Sathiyamoorthy, T.Vasudevan; Desalination, **164**, 111 **(2004)**.

[16] WY.Shih, K.Albrecht, J.Glater, Y.Cohen; Desalination, **169**, 213-221 **(2004)**.

[17] T.Alfrey, T.L.Young Jr; 'Copolymerization', Ed. G.E.Mam; Interscience Publ.: **(1964)**.

[18] NACE Standard, TM 0374-95, 'Test method for laboratory screening tests to determine the ability of scale inhibitors to prevent the precipitation of $CaSO_4$ and $CaCO_3$ from solution'.

[19] P.Shakkthivel, D.Ramesh, R.Sathiyamoorthi, T. Vasudevan; J.Appl.Polymer.Sci., **96**, 1451 **(2005)**.

[20] C.Gabrielli, M.Keddam, H.Perrot, A.Khalil, R. Rosset, M.Zidoune; J.Appl.Electrochem, **6**, 1125 **(1996)**.

[21] L.J.Simpson; Electrochemical Acta, **43**, 2543 **(1998)**.

[22] J.F.Yan, R.E.White, R.B.Griffin; J.Electrochem. Soc., **140**, 1275 **(1993)**.

[23] C.Gabrielli, M.Keddam, H.Perrot, A.Khalil, R. Rosset, M.Zidoune; J.Appl.Electrochem, **26**, 1125 **(1996)**.

[24] John Dyer; 'Application of Adsorption sspectroscopy of Organic compounds', 5th printing, Prentice-Hall of India Pvt Ltd., **4**, 23 **(1991)**.

[25] R.M.Silverstein, G.Glayton Bassler, TC.Morrill; 'Spectrometric Identification of organic compounds', 5th Edition, **(1961)**.

[26] P.Shakkthivel, T.Vasudean; Journal of Applied Polymer Science, **103(5)**, 3206 **(2007)**.

[27] J.F.Yan, T.V.Ngugen, R.E.White, R.B.Griffin; J. Electrochem.Soc., **140**, 733 **(1993)**.

[28] W.H.Hartt, D.H.Culberson, S.W.Smith; Corrosion, **40**, 609 **(1984)**.

[29] C.Deslouis, D.Festy, O.Gil, G.Rius, S.Touzain, B. Tribollet; Electrochimica Acta, **43**, 1891 **(1998)**.

[30] R.V.Lee, J.R.Ambrose; Corrosion, **44(12)**, 887 **(1988)**.

[31] J.Ledio, P.Leory, I.P.Labbe; TSM' eau, **(1985)**.

[32] C.Gabrieli, A.Khalil, P.Sakyat, C.Collin, R.Rosset; C.R.Acad.Sci: Paris, 315 Ser.II, 795 **(1992)**.

[33] C.Gabrielli, M.Keddam, A.Khalil, R.Rosset, M. Zidoune; Electrochimica Acta, **42(8)**, 1207 **(1997)**.

[34] Steven J.Severtson, Jihui Guo; J.Colloid and Inter. Sci., **246**, 423 **(2002)**.

[35] Per Kjellin; Colloids and Surfaces A:Physicochem. Eng.Aspects, **212**, 19-26 **(2003)**.

[36] C.Deslouis; C.Gabrielli, M.Keddam, A.Khalil, R. Rosset, B.Tribollet, M.Zidoune; Electrochimica Acta, **42(8)**, 1219 **(1997)**.

[37] C.Salam Joshep; 'Polymer Materials Encyclopedia', C.R.C.Press.Inc. Florida, 7587 **(1996)**.

[38] A.E.Austin, J.F.Miller, D.A.Vangham, J.F.Kircher; Desalination, **16**, 345 **(1975)**.

[39] E.Dalas, G.Koutsoukos Petros; Desalination, **78**, 403 **(1990)**.

[40] H.A.El Dahan,H.S.Hegazy; Desalination, **127**, 111 **(2000)**.

[41] E.R.Mc Cartnery, A.E.Alexander; J.Colloid and Interface Science, **13**, 383 **(1958)**.

[42] P.F.Rolfe; Desalination, **1**, 359 **(1960)**.

[43] C.H.Nestler; J.Colloid and Interface Science, **26**, 16 **(1958)**.

[44] P.Shakkthivel, T.Vasudevan; Desalination, **197 (1-3)**, 179 **(2006)**.